https://doi.org/10.20965/ijat.2023.p0305

Research Paper:

Machine Learning Based Position Prediction of a Target Tracked by Multi-Aperture Positioning System

Luis Garcia[*,,†], Uwe Bielke[***], Cornelius Neumann[**], and Rainer Börret[*]**

[*]Zentrum für Optische Technologien (ZOT), Aalen University
Beethovenstraße 1, Aalen, Baden-Württemberg 73430, Germany
[†]Corresponding author, E-mail: luis.garciabarth@hs-aalen.de
[**]Karlsruhe Institute of Technology (KIT), Karlsruhe, Germany
[***]Glasgow Caledonian University, Glasgow, United Kingdom
[Received October 31, 2022; accepted March 1, 2023]

This paper proposes a machine learning-based position prediction approach to determine the position of a light-emitting diode (LED) target using a new measuring system called the multi-aperture positioning system (MAPS). The measurement system is based on a photogrammetric approach using an aperture mask and a single camera sensor. To achieve high accuracy in position calculation, several complex algorithms with high computational complexity are used. The accuracy of the system is equal to or better than that of existing photogrammetric devices. We investigate whether a neural network (NN) can replace the algorithms currently used in the system software to increase the measurement frequency with similar accuracy. Simulated images are used to train the NN, while real images are used to measure performance. Previously, various algorithms were used to calculate the position of the target from the captured images. Our approach is to train an NN, using thousands of labeled images, to predict the position of the target from these images. We investigate whether systematic measurement errors can be avoided; not all factors affecting the measurement precision are yet known, can always be accurately determined, or change over time. When NNs are used, all information contained in the images is learned by the model, considering all influences present at the time of training. Results show that the trained NN can achieve similar performance to the previously used Gaussian algorithm in less time since no filters or other pre-processing of images are required. This factor directly affects the measurement frequency of the MAPS. The light spot center was detected with sub-pixel accuracy without systematic errors in contrast to some of the previously used algorithms. The simulation of the sensor images needs to be improved to investigate the full potential of the NN.

Keywords: photogrammetry, 3DOF measurement, machine learning, accuracy, online-calibration

1. Introduction

Machine tools, robots, and measuring machines can be found in almost all major industries today, such as the automotive industry, electronics manufacturing or component, and consumer goods production. As demand for individualized products increases and production runs shrink, multi-purpose machines are becoming increasingly important [1]. The ability to produce accurate parts is one of the most important performance criteria for modern production. Therefore, measuring machines are becoming increasingly important as the main tool for checking the dimensional accuracy of manufactured parts. Especially where high repeatability is required, measuring machines with high performance are indispensable. Owing to the demand for higher product quality, the improvement of measurement accuracy has become an extremely important area of research [2]. Increasing the accuracy of machines by correction can be done in two ways: either by correction in a feedback loop [3] or by calibration using a correction matrix [4]. Another important issue in modern production is the coordination of multiple machines working on a single task or workpiece. Their synchronization is crucial, otherwise they might fail. To avoid this, all machines and workpieces involved in the process must be precisely measured in the same coordinate system. Measuring machines available today, such as the laser trackers or camera-based systems, do not fulfill all of the following criteria: online measurement, high accuracy, and simultaneous measurement of multiple coordinate systems. Therefore, the multi-aperture positioning system (MAPS), a new photogrammetric measurement system presented by Bielke et al. [5], is developed. It consists of a camera sensor, an aperture mask, and a light-emitting diode (LED) target.

This study focuses on the development of a neural network (NN) to determine the centers of the light spots in the images taken by MAPS. This is the key step in calculating the position of the LED target using the MAPS software. The goal is to replace the traditionally used mathematical algorithms with an image regression NN. These have already proven themselves in a wide range of applications, from detecting and counting vehicles [6]

to quantifying cyanobacteria [7] or predicting the age of children's bones [8]. NNs are extremely versatile, using a function approximation to best map examples of inputs to examples of outputs [9].

Machine learning and NNs are also used in the robotics and other machine tool-related applications. Kato et al. used a random forest method to construct a calibration model for the positioning errors and to identify the positioning error factors [10]. For example, when robots handle heavy loads, their positioning accuracy often decreases. This has multiple causes, one of them is the errors caused by non-geometric parameters. It is possible to use a calibration routine based on an NN to improve the positioning accuracy of the robot by compensating for the aforementioned errors [11, 12]. Furthermore, NNs can also be used to identify positioning errors of industrial robots. Here, the NN learns from the tool center point (TCP) measurements of an external device and additional robot parameters [13, 14]. Mizutani et al. investigated the structure of deep NNs (DNN) used in triangulation displacement sensors. The information needed for the measurement was the position of the focused light intensity on a detector, similar to how MAPS works [15].

The remainder of this paper is structured as follows: We first describe the experimental setup, introducing the components. Thereafter, the methodology is introduced, and the necessary steps to calculate the position of the MAPS target are explained. This is followed by the simulation of the light spots and the training of the NN. The implementation of the NN and the critical aspects of this work are explained. In a first experiment, the sub-pixel accuracy of the NN is validated and compared to that of the current algorithms. Then the NN is trained and validated on a simulated image dataset, followed by real measured data.

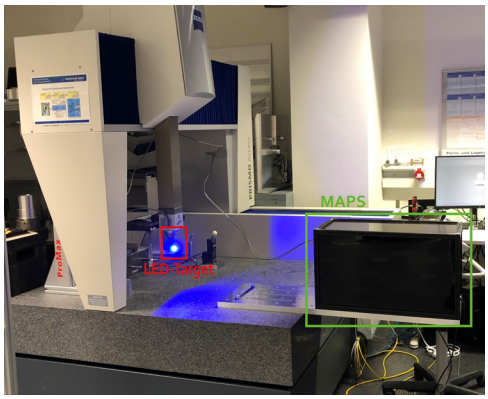

(a)

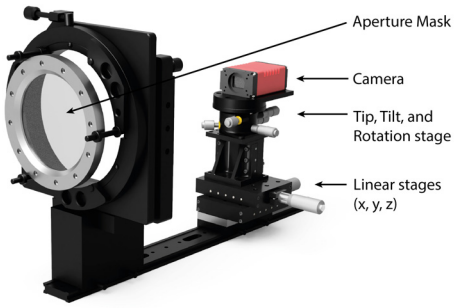

(b)

Fig. 1. MAPS experimental setup. (a) The setup is mounted on a Zeiss PRISMO Access. The LED-target is attached to a Zeiss VAST XT measurement head. The black box contains the MAPS setup, which protects it from stray light and dust. (b) Sketch of the MAPS setup inside the black box shown in (a). The camera is mounted on a tip, tilt, and rotation stages on three linear axes for a movement with 6DOF. It allows the adjustment of the camera sensor to the aperture mask.

2. Experimental Setup

The experimental setup is shown in **Fig. 1**. It consists of three main components—the MAPS measurement system, a coordinate measuring machine (CMM) (Zeiss PRISMO Access), and the proprietary software for simulation and NN engineering. MAPS consists of a high-resolution camera, Allied Vision Prosilica GT 3300 with 8.1 megapixels and 5.5 μm pixel pitch, operating at about 4 fps in this setup. In front of the camera is an aperture mask mounted. It is a glass disk covered with a chromium layer that contains approximately 40k aperture holes. This result in around 700 light spots projected onto the camera sensor. The greater the number of light spots, the more accurate the determination of the light source position is. As explained below, each pair of light spot and aperture hole forms a vector and they all ideally intersect at the same point—the location of the light source. The third component is the LED target, which is equipped with an ultra-bright blue LED. MAPS is mounted on the granite table of the CMM opposite the probe head, which is the LED target in this setup.

The CMM is used as a reference system for MAPS. It moves the LED target to defined coordinates while MAPS takes images at these positions. The images are stored and later used to train the NN. In addition, the MAPS software can simulate these exact images, which is explained later.

The simulation and NN training are performed on a desktop PC with an Intel i7-9700k, an NVIDIA 2070S, and 64 GB RAM running Windows 10. The NN is trained using the Keras Python library on the GPU. Both simulation and training are part of the in-house developed path correction and planning software (PCAPS).

3. Methodology

To determine the position of the light source, MAPS executes a sequence of different algorithms on the captured images. An image represents a matrix of light spots mapped by the light from the LED target passing through the holes in the aperture mask and hitting the camera sensor. To calculate the position of the LED target from these images, the following steps are required [16]:

1. First, Gaussian blur and Fourier filter are applied to the image to improve the performance (reducing the standard deviation) of the spot center algorithms, followed by a threshold filter, which allows the light spots to be distinguished from the rest of the image via edge detection.

2. A peak-finding algorithm is used to find the center of each spot. Currently, a Gaussian fitting algorithm [17] or the method of moments (MoM) [18] can be used for this. For real measurement tasks, only the MoM algorithm is currently used, since the Gaussian algorithm requires too much computing time.

3. The program identifies the marker in the image, which is used to determine the illuminated apertures on the mask. This is necessary to combine the light spots with aperture holes in the next step.

4. Finally, a vector is defined from the center of each light spot through the corresponding aperture hole in the mask (approximately 700 in total), after which their intersection point can be calculated to represent the actual position of the light source.

The main challenge is to determine the centers of the light spots. The current state-of-the-art method uses two different algorithms for this purpose. While the Gaussian algorithm is accurate and slow, the MoM algorithm is fast but less accurate. Since the accuracy in determining the center position of the spots directly affects the final calculated LED position, an algorithm that is as accurate as possible is required. Nevertheless, it should also be as fast as possible to avoid losing measurement speed. For this reason, a new approach for determining the spot center using NN is presented in this paper. This means the algorithm in step 2 is replaced by a trained NN and step 1 can be skipped completely as it does not affect accuracy [19].

3.1. Parameters Influencing the Measurement Uncertainty

One of the most important factors is the distance between the LED target and the detector. As the distance increases, the changes in the image become smaller and more difficult to detect. The measurement uncertainty increases because the influence of the disturbance variables increases as a result. For example, the intensities of the light spots decrease and they get smaller because less light reaches the sensor with the increase in LED distance. The spot shape also changes with the increase in distance. MAPS operates in the near field (LED distance to detector < 700 mm), for greater distances Fresnel diffraction must be considered. The interference starts very small but increases with distance. The actual spot shape will no longer be Gaussian-like, but Fresnel-like. This is one of the reasons why the Gaussian algorithm is less accurate at greater light source distances. Another reason is that the image noise (caused by natural camera sensor noise) gets more relevant when the overall intensities of the spots decreases. This makes it harder for the algorithms to determine the center within sub-pixel accuracy. The noise changes with the temperature of the camera sensor, therefore it is very important to run MAPS in a room with regulated air temperature.

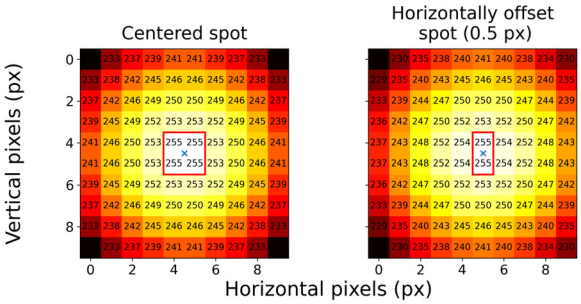

Fig. 2. Visualization of the sensor pixel intensity of a simulated light spot (center section 10×10 pixels). Two spot images are shown: one with the spot center in the middle of the image (left) and another where the spot center is offset horizontally by 0.5 pixels (right). Each rectangle represents one pixel, with the numeric value indicating the respective 8 bit intensity value. The brightest pixels are framed, and the center of the spot is marked with a cross.

Another important influencing factor is the available number of pixels per spot. The more pixels a spot has, the more precisely its center can be determined. This is related to the LED distance, the size of the sensor, the chamber constant (distance between sensor and aperture mask), the aperture size, and the pixel pitch of the sensor. In terms of the NN, the number of simulated images used for training affects the measurement uncertainty. The more the training data, the more accurate the NN prediction model.

3.2. Sub-Pixel Accuracy

For MAPS to achieve high accuracy, it is important to precisely determine the centers of the light spots. As mentioned before, this means sub-pixel accuracy or, in other words, with a resolution greater than the pixel size of the sensor (5.5 μm). Since the light spots are Gaussian-like distributed, the point with the highest intensity value is considered the center of the spot. This can be illustrated by simulating a spot image. One where the center of the light spot is in the center of the image, and another where the center of the light spot is offset by 0.5 pixels. **Fig. 2** shows the 10×10 pixel center area of such an image. The intensity value (8 bits) is written in the pixels, the brightest pixels are framed, and the spot center is marked with a cross. In the left image with the centered spot, there are four pixels with a maximum intensity of 255, which means that the spot center is in their midst. If the spot center is shifted horizontally by 0.5 pixels, the intensity distribution is that in the right image is obtained. There are now only two pixels with the maximum intensity, so the spot center is in their midst.

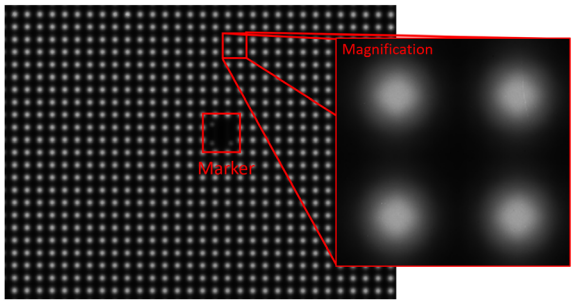

Fig. 3. Actual image taken by MAPS at an LED distance of 260 mm from the sensor. The magnification shows four light spots, where the Gaussian distribution can be seen more clearly. The two-by-two spot-sized area in the middle of the image, with some smaller light spots, is the marker. It is used to determine the section of the aperture mask displayed on the camera sensor.

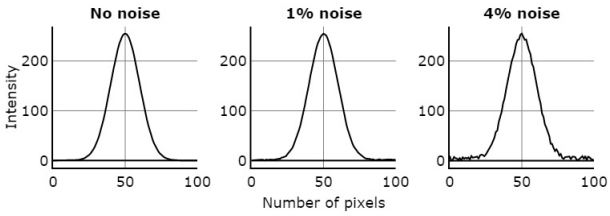

Fig. 4. Intensity diagram of the simulated spots with different random noise levels of 0%, 1%, and 4%. A noise level of 4% is close to the real camera sensor noise and therefore ideal to represent the spots. The y-axis represents the pixels (8 bit) intensity (arbitrary units), the x-axis shows the number of pixels in the spot.

This is just a very simplified example of how the intensity distribution changes when the center moves. But it is important to understand that its position depends on the position of the light source relative to the detector and that it is necessary to determine the position of the center as accurately as possible.

3.3. NN Approach

Since MAPS images have a high resolution of 3296 × 2472 pixels with a depth of 8 bits, huge hardware resources, especially video RAM, are required. Reducing the size is not an option because the relevant information is lost and the NN cannot learn the relationship between the input and output. Subdividing the image into smaller sections is also not an option, otherwise the relationship between the spots and the aperture holes will be lost, not to mention that the number of combined spots is directly related to the accuracy of the LED position determination.

Each MAPS image is a matrix of light spots, as shown in **Fig. 3**. The concept is to first cut out all light spots from the image and save them with their corresponding spot centers and then train the NN on that data and use the trained NN model as a spot center determination algorithm replacing the algorithms currently used. In this way, the entire image can be divided into approximately 700 smaller images, reducing the hardware resources required. The NN is trained on simulated light spots whose center positions are known, rather than on real spots. Since the centers of the real light spots are unknown, only the algorithms currently in use can calculate them. If this information is used to label the images and the NN is trained on them, it may never outperform the traditionally used algorithms. It is important to note that the NN must achieve sub-pixel accuracy in determining the spot center, just like the current algorithms.

3.4. Light Spot Simulation for Different Noise Levels

The light spot simulation is a crucial part of this study, as the NN is supposed to learn from the simulated data. The data should be as close to the real light spot images as possible to ensure good performance later on. The simulation was implemented in PCAPS where all the image and spot parameters, as well as the random sensor noise and various filters can be set. The number of images generated depends on the number of spot center positions given in the simulation. These positions are interpreted as offset values to the center of the simulated image. The light spots in the simulation are approximated using a two-dimensional Gaussian function according to Eq. (1) [20]:

$$f(x,y) = A\exp\left(-\left(\frac{(x-x_0)^2}{(2\sigma_x^2)} + \frac{(y-y_0)^2}{(2\sigma_y^2)}\right)\right), \quad (1)$$

where x_0 and y_0 are the center coordinates of the spot. By adding an offset value to these, for example 0.1, it is possible to shift the center in any directions with sub-pixel accuracy. The smaller the offset steps, the more the generated spots and the bigger the dataset.

For this experiment, three datasets with different levels of image noise (0%, 1%, and 4%) were generated with 10k samples each. A noise level of 4% ideally represents the real images, the optimal image has no noise, and 1% is chosen to represent images with minimal noise. The image noise level increases mainly with the sensor temperature. Preliminary tests have shown that with proper sensor cooling, a noise level of $\leq 4\%$ is realistic.

The difference between the noise levels can be seen in **Fig. 4**. To keep this experiment simple, the center of the spot is shifted only in positive x-direction by 0 to 1 pixel with a step size of 0.0001 pixels. In addition, a random noise of 0%–10% of the step size is added to the offset values so that the images in the dataset are not equally distributed. Both, the MoM and Gaussian algorithms are used to calculate the spot centers, which serve as references. The goal of this experiment is to determine the sub-pixel accuracy of the NN at different noise levels and compare it with that of the other algorithms.

3.5. Creating MAPS Image Datasets

After investigating the sub-pixel accuracy of the NN at different noise levels, an entire MAPS image dataset was

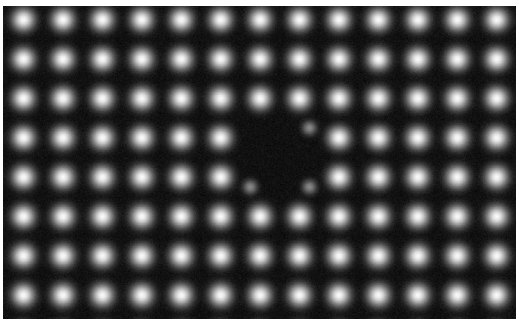

Fig. 5. Section of a simulated MAPS image with 4% noise, including a marker. The image is created by simulating the individual light spots created by light rays traveling through the aperture mask and hitting the camera sensor.

created by simulation. For this purpose, a real measurement experiment was first performed with MAPS, where the position of the light source (mounted on the CMM) was measured at different positions on the optical axis of MAPS (z-axis). The CMM moved the light source from position $P_{start} = 250$ mm to $P_{end} = 950$ mm with a step size of 1 mm. Ten measurements per position were taken. To keep the number of measurements within limits, a 1-D path was chosen over a 3-D one. The optical axis was chosen because these are the most critical measurement points for MAPS. Longitudinal displacement of the light source is much harder to detect than lateral displacement. The image changed comparatively little due to the small angular change between the light source and the apertures. The idea behind this is that if the NN achieves good results here, at least the same performance should be achieved with full measurement volume and the same measurement data resolution.

After that, the same experiment was simulated, or more precisely, the images were simulated. The simulation also generated ten images for each mm. In total, 7000 images were simulated and separated into approximately six million spot images. It was based on the spot-image simulation and the same procedure was performed for all the apertures of the mask. By calculating the apertures that would hit the sensor, a whole measured image could be simulated, including the markers, as shown in **Fig. 5**. The simulation was implemented in PCAPS, where the position of the light source, aperture mask, and camera could be set. This made it possible to reproduce the real experimental setup in the software. By moving the position of the artificial light source, it was possible to simulate the movement of the real light source.

For both the real measurement and simulation, the spots were extracted from the measured images and stored individually, including the spot centers stored in a text file. For the simulation, the (ideal) simulated spot centers were used, and for the real measurement, the spot centers calculated by the Gaussian algorithm were used. Using this data, the NN was trained later, and the prediction was compared with the other two algorithms.

3.6. NN Preparation and Training

The NN used in the experiments was based on the one presented by Rosenfelder et al. [21]. It was an image regression NN, which means that it takes an image as input and outputs a numerical value. In our case, a spot center image was the input and the position (x, y values) of the spot center was the target feature. Thus, the NN predicted two numerical values. It was implemented in the existing MAPS software package, PCAPS. Thus, not only the NN can be trained directly on the images taken by MAPS, but the trained model can also be used as a method for determining the spot centers in the images in addition to the Gaussian and MoM algorithms. The calculation of the position of the light source is then based on the prediction of the NN.

The data preparation was kept simple, since complex data enhancement does not bring great advantages, as shown by the first investigations. Scaling, stretching, rotation, or convolution manipulation could not be used as this could lead to a different valid image. Owing to the size of the image and the limited video RAM, it was not possible to input the entire MAPS image into the network. Therefore, in the pre-processing step, the spots were cut out of the image and each one was stored separately along with the corresponding center coordinates. The NN was then trained on them, while the Gaussian and MoM algorithms continued to use the entire images. The same applied for prediction. Each spot was be cropped from the taken image for the network to make a prediction. However, this step was not really different from the one done before in the other algorithms, where, first the spots must be located in the image to make it possible to calculate their centers.

The NN was trained using each of the datasets individually, with the weights subsequently stored. The datasets were divided into three categories as follows: 70% training data, 20% validation data, and 10% test data. The best performing hyperparameter values of the network were determined by the design of experiments and the subsequent training and validation of the NN on the datasets. Early stopping was enabled to prevent the network from overfitting.

4. Experimental Results

The following section describes the experimental results. It is divided into three subsections. First, the sub-pixel accuracy of the three algorithms for different image noise levels is discussed. Then, the performance of NN in predicting the spot centers of a simulated dataset is shown. Finally, the prediction for a real image dataset is demonstrated.

4.1. Performance Comparison of the Algorithms at Different Noise Levels

Testing the algorithms for sub-pixel accuracy clearly shows the advantage of the Gaussian algorithm over the MoM, as it is observed that the Gaussian algorithm has

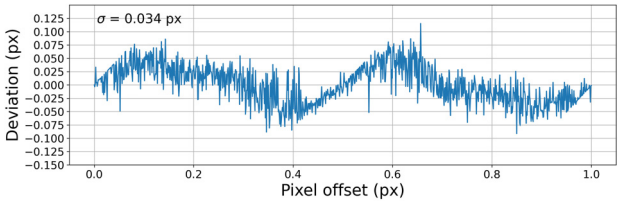

(a) MoM algorithm

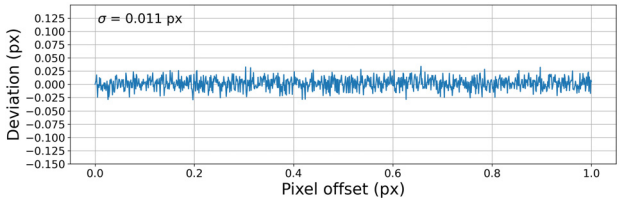

(b) 2D Gaussian algorithm

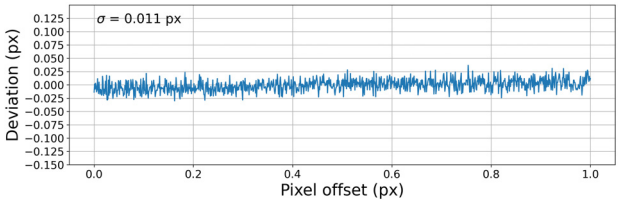

(c) NN prediction

Fig. 6. Deviation of the calculated spot center from the actual one given by the three algorithms on simulated spot images. In the simulation, the spot center is shifted between 0 and 1 pixel in the positive x-direction in the images. A step size of 0.0001 is chosen, which generates 10k images. For every image, the spot center is calculated or predicted.

no systematic error. In **Fig. 6**, the graphs show the deviation in pixels for the simulated pixel offset values (0 to 1) for the three algorithms. The graph of the NN deviation also shows no systematic error. The standard deviation of the NN prediction is almost as small as that of the Gaussian algorithm; this is achieved without pre-processing the images with filters, which is necessary for the other algorithms to achieve this level of performance. The impact of filters on the accuracy of these algorithms was investigated in a previous study by Garcia et al. [19].

The graphs in **Fig. 6** show only the results for the dataset with 4% image noise as an example to visualize systematic and random errors. **Table 1** shows the performances in terms of standard deviation for all datasets.

At a noise level of 4%, the NN and Gaussian algorithms have a similar standard deviation and outperform the MoM algorithm by approximately three times. Since the dataset with 4% noise best represents the real data, this is the most important column. Having an NN that can predict the center of the light spot with approximately the same accuracy as the previously used algorithms is an important foundation for the next experiments.

The performances of all three algorithms improve as expected at lower noise levels. The NN is even slightly more accurate at 1% noise than at 0%. At 0% noise, the Gaussian algorithm does not show any deviation since a Gaussian fit to an ideal Gaussian distributed spot is used.

Table 1. Comparison of different methods for determining the spot center position offset in simulated images. Each method is evaluated by the test dataset described in Section 3.4. The table shows the standard deviation in pixels for each method at different noise levels.

	0% noise	1% noise	4% noise
NN	0.0071	0.0060	0.0110
MoM	0.0233	0.0377	0.0342
Gaussian	0	0.0026	0.0107

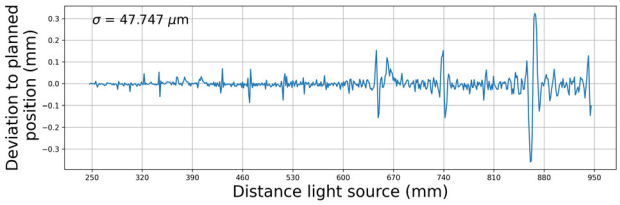

(a) MoM algorithm

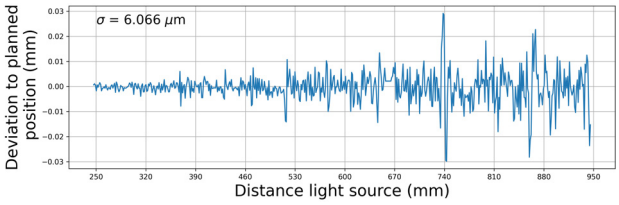

(b) 2D Gaussian algorithm

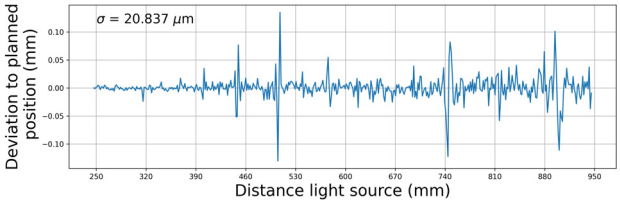

(c) NN prediction

Fig. 7. The deviation between the calculated and the actual simulated position of the light source, one graph for each algorithm. In the simulation, the light source is moved in a positive direction on the optical axis of MAPS. Starting at 250 mm from the sensor up to 950 mm. Ten images are simulated every 1 mm.

4.2. NN Prediction on Simulated Images

Using the same NN architecture as in the previous experiment, training was performed on a fully simulated dataset. The dataset was created as described in Section 3.5. The trained NN, MoM, and Gaussian algorithms were then used to compute the position of the light source from the images. In **Fig. 7**, the deviation of the calculated light source position from the actual simulated position is shown, one graph for each algorithm.

A closer look at the diagrams (a) and (c) reveals periodic outliers, ranging from 50 μm up to 300 μm for the MoM algorithm and up to 120 μm for NN. Some of them occur at the same position for all algorithms and can also be observed for the Gaussian algorithm, where the maximum value is much smaller at 30 μm and can hardly

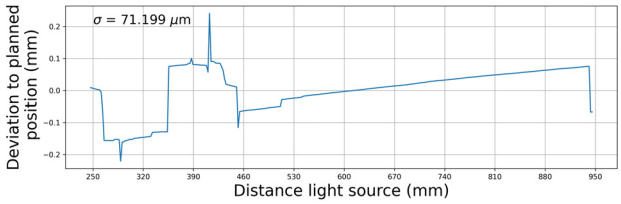

Fig. 8. The deviation between the predicted NN light source position and that of the CMM. In the experiment, the light source is moved in the positive direction on the optical axis of MAPS, starting at a distance of 250 mm from the sensor and increasing to 950 mm. Ten images are taken every 1 mm, and the position of the light source is predicted by the NN trained on simulated images.

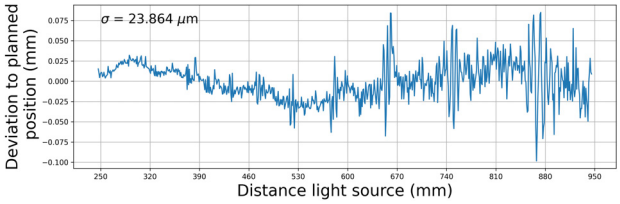

(a) MoM algorithm

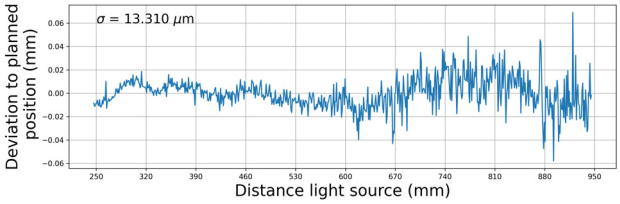

(b) 2D Gaussian algorithm

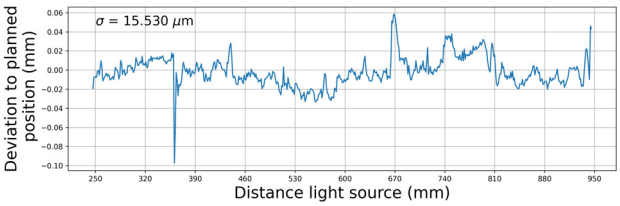

(c) NN prediction

Fig. 9. The deviation between the calculated light source position and that of the CMM. In the experiment, the light source is moved in the positive direction on the optical axis of the MAPS. Starting with a distance of 250 mm from the sensor up to 950 mm. Ten images are taken every 1 mm.

be distinguished from the random error. The current theory is that, in some measured images, the spots have a very similar intensity distribution, resulting in an incorrectly calculated center coordinates, hence the outliers in the deviation graph. This can occur especially when the light source is moved along the optical axis of MAPS, since the angle between the light source and the detector changes only slightly at different distances. It should also be remembered that the simulated images are created more or less systematically, which makes it more plausible that NN has a systematic error in its predicted values.

Since there are fewer outliers in the graph of the Gaussian algorithm, the standard deviation σ is much smaller at around 6 μm. For the other two algorithms on the other hand, the peaks, considered systematic errors, are much bigger than the random error. Therefore, the standard deviation is greater, with around 21 μm for NN and 48 μm for the MoM.

4.3. NN Prediction on Real Images

The NN trained on the simulated dataset from the previous experiment was used to predict the spot centers of real MAPS images. Then, again, the position of the light source was calculated. The real dataset was created as described in Section 3.5. **Fig. 8** shows the deviation between the calculated and the real light source position (CMM position is used as the reference).

There is a large systematic error in the deviation plot. There are outliers and two plateaus in the first section (250–450 mm distance), where the deviation is between negative 150 μm and positive 100 μm. From 450 mm to 950 mm, the deviation value increases almost linearly from a negative 100 μm to positive 100 μm. A deviation close to zero cannot be observed (except for some single measurement positions), and the result is not comparable with those of the other algorithms.

This kind of systematic error is an indicator that the NN has not learned the relevant information from the simulated images to make an accurate prediction on the real images. This, in turn, means that the simulated data are not similar to the real data enough to be used as training data.

In its current state, the simulation does not consider changes in spot brightness, which occurs when the distance of the light source from the sensor changes. This results not only in a change in the spot size (smaller at greater distance), but also in a change in its distribution and their distance to each other. The real spots are only Gaussian-like, not exactly Gaussian-distributed, as assumed in the simulation. In reality, the shape of the spot changes slightly when the light source is moved further away from the aperture mask.

Since MAPS operates in the near field (Fresnel diffraction), the spots are expected to have a more Fresnel-like shape for more distant positions. Especially when the criteria for spatial coherence are met, as mentioned earlier. Given this, the NN might mistake a first-order peak for the center of the spot, resulting in an incorrectly calculated position. This and the limitations of the simulation mentioned above cause the large systematic error in the calculation of the light source position.

In the last experiment, NN is trained directly on the acquired MAPS images. Again, the spot centers were predicted, and the position of the light source was calculated. The deviation from the CMM position was calculated for all three algorithms and is shown in **Fig. 9**. The plot of the NN deviation shows the same low-frequency systematic error as the other two plots. This is not surprising since the spot centers determined by the Gaussian algorithm were used to label the real image data. These systematic errors

are considered an axis drift and were explained by Bielke et al. [5].

The NN plot appears to be less noisy because the random error has a lower frequency, but the noise has the same level as that in the Gaussian plot. The standard deviation is comparable to that of the Gaussian and MoM algorithms. The outlier at 360 mm is probably a major misprediction of the NN or a missing measurement value.

Since NN was trained on the Gaussian algorithm data, the position predicted by NN cannot be directly compared to the Gaussian or MoM algorithm calculations. Instead, this experiment proves that NN learns the relevant information from the images when they are provided. It predicts the spot centers with acceptable accuracy, similar to the performance of the Gaussian algorithm.

5. Conclusion

This study presents a novel approach for calculating the position of the MAPS LED target using NN to predict the light spot centers. A proprietary simulation software is used to generate artificial MAPS image datasets. NN is tested for sub-pixel accuracy in the first experiment, showing no relevant systematic error in the prediction of the light spot centers. In the second experiment, NN is trained and validated on a full simulated dataset, showing performance comparable to the Gaussian and MoM algorithms. The trained NN is then used to predict the spot centers from real image data, but it does not perform sufficiently well owing to large systematic errors in the calculated light source position. Therefore, NN is trained directly on the real image data and validated on a test set. This makes the prediction more accurate, and the computed position has no unexpected systematic errors.

Although the light spots generated by the simulation are very similar to the real ones, this only applies to the calculation by the traditionally used algorithms and not to NN. Therefore, they are not optimal for training NN and making predictions for real light spots. To enhance the performance, first, the simulation must be extended. Important additions are the spot size, intensity distribution, and spot shape. Then, the right amount of data must be selected to retrain and validate NN on real images. This study proves that a trained NN can achieve similar performance to the previously used Gaussian algorithm. It is worth noting that NN does this in less time (the computation time is less because NN is optimized for the GPU, and no filters or other pre-processing of the images are required). This is indeed an important factor, as it directly affects the measurement frequency of MAPS. Detection of the light spot center with sub-pixel accuracy is also possible without systematic errors, in contrast to the MoM algorithm. The full potential of NN has yet to be explored. Regarding systematic errors, further investigation could be very promising.

In future work, the simulation should be improved, and a larger variety of data should be simulated (e.g., a 3-D measurement volume). The simulated data should be as close to real images as possible so that the NN can learn all relevant information. Only then can the prediction results be used to accurately calculate the position of the light source.

Acknowledgments

This research was funded by the German Research Foundation (DFG) ("Precise, flexible, and modular 6-dimensional additive manufacturing platform including individual in-situ analysis," contract number BO 3489/1-2). The author's would like to thank the German Federal Ministry for Economic Affairs and Energy and the German Research Foundation for funding this research.

References:

[1] H. Schwenke, W. Knapp, H. Haitjema, A. Weckenmann, R. Schmitt, and F. Delbressine, "Geometric Error Measurement and Compensation of Machines—An Update," CIRP Annals, Vol.57, No.2, pp. 660-675, 2008.

[2] P. S. Huang and J. Ni, "On-Line Error Compensation of Coordinate Measuring Machines," Int. J. of Machine Tools and Manufacture, Vol.35, No.5, pp. 725-738, 1995.

[3] H. Kunzmann, T. Pfeifer, R. Schmitt, H. Schwenke, and A. Weckenmann, "Productive Metrology – Adding Value to Manufacture," CIRP Annals, Vol.54, No.2, pp. 155-168, 2005.

[4] S. Sartori and G. X. Zhang, "Geometric Error Measurement and Compensation of Machines," CIRP Annals, Vol.44, No.2, pp. 599-609, 1995.

[5] U. Bielke, L. Garcia, D. K. Harrison, T. Hageney, K. Banzhaf, E. Wiedenmann, and R. Börret, "New photogrammetric approach for measuring the position of a Tool-Center-Point," 41st MATADOR Conf. on Advanced Manufacturing, 2021.

[6] H. Tayara, K. G. Soo, and K. T. Chong, "Vehicle Detection and Counting in High-Resolution Aerial Images Using Convolutional Regression Neural Network," IEEE Access, Vol.6, pp. 2220-2230, 2018.

[7] J. C. Pyo, H. Duan, S. Baek, M. S. Kim, T. Jeon, Y. S. Kwon, H. Lee, and K. H. Cho, "A Convolutional Neural Network Regression for Quantifying Cyanobacteria Using Hyperspectral Imagery," Remote Sensing of Environment, Vol.233, 111350, 2019.

[8] X. Ren, T. Li, X. Yang, S. Wang, S. Ahmad, L. Xiang, S. R. Stone, L. Li, Y. Zhan, D. Shen, and Q. Wang, "Regression Convolutional Neural Network for Automated Pediatric Bone Age Assessment from Hand Radiograph," IEEE J. of Biomedical and Health Informatics, Vol.23, No.5, pp. 2030-2038, 2019.

[9] I. Goodfellow, Y. Bengio, and A. Courville, "Deep Learning," The MIT Press, 2016.

[10] D. Kato, K. Yoshitsugu, N. Maeda, T. Hirogaki, E. Aoyama, and K. Takahashi, "Positioning Error Calibration of Industrial Robots Based on Random Forest," Int. J. Automation Technol., Vol.15, No.5, pp. 581-589, 2021.

[11] Y. Wang, Z. Chen, H. Zu, X. Zhang, C. Mao, and Z. Wang, "Improvement of Heavy Load Robot Positioning Accuracy by Combining a Model-Based Identification for Geometric Parameters and an Optimized Neural Network for the Compensation of Nongeometric Errors," Complexity, Vol.2020, 5896813, 2020.

[12] S. Aoyagi, M. Suzuki, T. Takahashi, J. Fujioka, and Y. Kamiya, "Calibration of Kinematic Parameters of Robot Arm Using Laser Tracking System: Compensation for Non-Geometric Errors by Neural Networks and Selection of Optimal Measuring Points by Genetic Algorithm," Int. J. Automation Technol., Vol.6, No.1, pp. 29-37, 2012.

[13] D. Kato, K. Yoshitsugu, T. Hirogaki, E. Aoyama, and K. Takahashi, "Predicting Positioning Error and Finding Features for Large Industrial Robots Based on Deep Learning," Int. J. Automation Technol., Vol.15, No.2, pp. 206-214, 2021.

[14] G. Zhao, P. Zhang, G. Ma, and W. Xiao, "System Identification of the Nonlinear Residual Errors of an Industrial Robot Using Massive Measurements," Robotics and Computer-Integrated Manufacturing, Vol.59, pp. 104-114, 2019.

[15] Y. Mizutani, S. Kataoka, Y. Nagai, T. Uenohara, and Y. Takaya, "Structure Estimation of Deep Neural Network for Triangulation Displacement Sensors," CIRP Annals, Vol.71, No.1, pp. 425-428, 2022.

[16] U. Bielke, L. Garcia, D. K. Harrison, T. Hageney, K. Banzhaf, E. Wiedenmann, and R. Börret, "Simulation and Accuracy Evaluation of a New 3D Photogrammetric Position Measurement System," euspen's 22nd Int. Conf. & Exhibition, 2022.

[17] N. Hagen and E. L. Dereniak, "Gaussian Profile Estimation in Two Dimensions," Applied Optics, Vol.47, No.36, pp. 6842-6851, 2008.
[18] K. O. Bowman and L. R. Shenton, "Estimator: Method of Moments," S. Kotz, C. B. Read, and D. L. Banks (Eds.), "Encyclopedia of Statistical Sciences," pp. 2092-2098, Wiley, 1998.
[19] L. Garcia, U. Bielke, C. Neumann, T. Hageney, K. Banzhaf, E. Wiedenmann, and R. Börret, "Machine-Learning-Ansatz zur Bestimmung der Target-Position eines optischen Messgeräts," T. Luhmann and C. Schumacher (Eds.), "Photogrammetrie – Laserscanning – Optische 3D-Messtechnik: Beiträge der Oldenburger 3D-Tage 2022," pp. 33-42, Wichmann Verlag, 2022 (in German).
[20] G. L. Squires, "Practical Physics," Cambridge University Press, 2001.
[21] M. Rosenfelder, "Transfer Learning with EfficientNet for Image Regression in Keras – Using Custom Data in Keras," 2020. https://rosenfelder.ai/keras-regression-efficient-net/ [Accessed January 1, 2022]

Name:
Luis Garcia

ORCID:
0000-0002-6628-817X

Affiliation:
Research Scientist, Zentrum für Optische Technologien (ZOT), Aalen University

Address:
Anton-Huber-Straße 25, Aalen, Baden-Württemberg 73430, Germany

Brief Biographical History:
2018 Received B.Eng. degree from Esslingen University
2019 Received M.Sc. degree from Aalen University
2022- Ph.D. Student, Karlsruhe Institute of Technology (KIT)

Main Works:
• "Machine-Learning-Ansatz zur Bestimmung der Target-Position eines optischen Messgeräts," T. Luhmann and C. Schumacher (Eds.), "Photogrammetrie – Laserscanning – Optische 3D-Messtechnik: Beiträge der Oldenburger 3D-Tage 2022," pp. 33-42, Wichmann Verlag, 2022 (in German).
• "Online Position Correction Approach of an Industrial Robot by Using a New Photogrammetric Measurement System," Proc. of the Institution of Mechanical Engineers, Part B: J. of Engineering Manufacture, 09544054221131156, 2022.

Name:
Uwe Bielke

ORCID:
0000-0002-8329-0810

Affiliation:
Research Scientist, Zentrum für Optische Technologien (ZOT), Aalen University

Address:
Anton-Huber-Straße 25, Aalen, Baden-Württemberg 73430, Germany

Brief Biographical History:
2012 Received B.Eng. degree from Aalen University
2018 Received M.Sc. degree from University of Stuttgart
2019- Ph.D. Student, Glasgow Caledonian University

Main Works:
• "New photogrammetric approach for measuring the position of a Tool-Center-Point," 41st MATADOR Conf. on Advanced Manufacturing, 2021.
• "Simulation and Accuracy Evaluation of a New 3D Photogrammetric Position Measurement System," euspen's 22nd Int. Conf. & Exhibition, 2022.

Name:
Cornelius Neumann

Affiliation:
Professor and Head, Lighting Technology Department (LTI), Karlsruhe Institute of Technology (KIT)

Address:
Geb. 30.34, Engesserstraße 13, Karlsruhe, Baden-Württemberg 76131, Germany

Brief Biographical History:
1998- Hella GmbH & Co. KGaA
2009- Director, Forschungsinstitut für automobile Lichttechnik und Mechatronik (L-LAB)
2009- Professor, KIT

Main Works:
• "Symmetry Breaking in Crossed Magnetic and Electric Fields," Physical Review Letters, Vol.78, No.25, pp. 4705-4708, 1997.
• "Development in illumination optics," Advanced Optical Technologies, Vol.5, No.2, p. 107, 2016.

Name:
Rainer Börret

ORCID:
0000-0002-2550-2088

Affiliation:
Professor and Head, Zentrum für Optische Technologien (ZOT), Aalen University

Address:
Beethovenstraße 1, Aalen, Baden-Württemberg 73430, Germany

Brief Biographical History:
1990- Scientific Project Manager for the fabrication and metrology of space optics, Carl Zeiss AG
1996- Program Manager 193 nm, Carl Zeiss SMT GmbH
2003- Professor, Aalen University

Main Works:
• "Current Voltage Characteristics of a Gas Field Ion Source with a Supertip," J. of Physics D: Applied Physics, Vol.23, No.10, pp. 1271-1277, 1990.
• "ASPHERO5 – Simulation and Analysis of the Aspherical Polishing Process," Key Engineering Materials, Vols.364-366, pp. 488-492, 2008.
• "Online Position Correction Approach of an Industrial Robot by Using a New Photogrammetric Measurement System," Proc. of the Institution of Mechanical Engineers, Part B: J. of Engineering Manufacture, 09544054221131156, 2022.